

1 Chemometric processing of second-order liquid
2 chromatographic data with UV-visible and
3 fluorescence detection. A comparison of multivariate
4 curve resolution and parallel factor analysis 2

5
6 *Santiago A. Bortolato, Alejandro C. Olivieri**

7
8 Departamento de Química Analítica, Facultad de Ciencias Bioquímicas y Farmacéuticas,
9 Universidad Nacional de Rosario e Instituto de Química Rosario (IQUIR-CONICET), Suipacha
10 531, S2002LRK Rosario, Argentina.

11
12 * Corresponding author. Tel/ Fax: +54 341 4372704. E- mail: olivieri@iquir-conicet.gov.ar.

15 **ABSTRACT**

16 Second-order liquid chromatographic data with multivariate spectral (UV-visible or
17 fluorescence) detection usually show changes in elution time profiles from sample to sample,
18 causing a loss of trilinearity in the data. In order to analyze them with an appropriate model, the
19 latter should permit a given component to have different time profiles in different samples. Two
20 popular models in this regard are multivariate curve resolution-alternating least-squares (MCR-
21 ALS) and parallel factor analysis 2 (PARAFAC2). The conditions to be fulfilled for successful
22 application of the latter model are discussed on the basis of simple chromatographic concepts.
23 An exhaustive analysis of the multivariate calibration models is carried out, employing both
24 simulated and experimental chromatographic data sets. The latter involve the quantitation
25 of benzimidazolic and carbamate pesticides in fruit and juice samples using liquid
26 chromatography with diode array detection, and of polycyclic aromatic hydrocarbons in water
27 samples, in both cases in the presence of potential interferents using liquid chromatography with
28 fluorescence spectral detection, thereby achieving the second-order advantage. The overall
29 results seem to favor MCR-ALS over PARAFAC2, especially in the presence of potential
30 interferents.

31

32 *Keywords:* Parallel factor analysis 2; Multivariate curve resolution-alternating least-squares;
33 Non-trilinear chromatographic data; Polycyclic aromatic hydrocarbons; Pesticides; Second-order
34 advantage.

35

36 1. INTRODUCTION

37 The increasing analytical interest in second-order liquid chromatographic data with
38 multivariate (UV-visible or fluorescence) detection is due to the fact that by suitable processing
39 them with chemometric algorithms, analyte quantitation is possible in the presence of potential
40 interferences (exploiting the so-called second-order advantage), and using simple chromatographic
41 systems which save experimental time and organic solvents [1-5]. It is apparent that the
42 integration of multiple data sets into one coherent computational model offers theoretical and
43 practical advantages from an analytical point of view [6-8]. Although many applications of
44 second-order multivariate calibration to chromatographic information have been developed, an
45 important challenge for these approaches still remains: the existence of temporal misalignment in
46 the data [9,10], meaning that a given constituent peak in different chromatographic runs appears
47 at different positions and/or with different shapes along the elution time axis. Technically, this
48 situation is described as leading to a loss of the property of trilinearity in the data, which
49 basically requires that each chemical component should present a unique profile (both in the
50 spectral and elution time mode) in all samples [11]. In the case of non-trilinear chromatographic
51 data, two alternatives are available for data processing: (1) employ flexible algorithms, which
52 permit a given component to have different time profiles in different samples, such as parallel
53 factor analysis 2 (PARAFAC2) [12-14] and multivariate curve resolution-alternating least-
54 squares (MCR-ALS) [15-18], and (2) mathematically pre-process each data matrix so that the
55 analyte peaks are properly aligned and trilinearity is restored, and methods such as classical
56 PARAFAC [9] or trilinear evolving factor analysis (TEFA) [19] can be applied. The latter
57 option, however, does not appear to be the universal answer to the present problem, principally
58 for three reasons: (1) the alignment methods are mostly developed for vectors (chromatographic

59 traces with univariate detection) and not for matrices, (2) they are sometimes difficult to
60 implement due to the large number of subtle theoretical details which must be considered [20-
61 22], and (3) when unexpected constituents appear in test samples, or in the presence of peak
62 swapping, many of these algorithms run into problems [20]. In short, there are many available
63 and wildly different alignment methods, so that, according to ref. [20] it is necessary to have *a*
64 *set of rules-of-thumb that specify when to use which warping method, with what criterion, and*
65 *how to choose the optimal reference.*

66 In the case of flexible algorithms for matrix chromatographic data processing,
67 PARAFAC2 and MCR-ALS have shown good analytical performance to solve analytical
68 problems of diverse natures [23-27]. PARAFAC2 is a variant of the well-known trilinear
69 PARAFAC model, but does not assume a common shape for the elution profile of a given
70 component in each sample [28,29]. One appealing feature of PARAFAC2 is that it often leads to
71 unique solutions. However, this comes at the expense of a specific algorithmic restriction, to be
72 explained in detail below, which does not appear to represent, in general, a real chromatographic
73 system.

74 On the other hand, MCR-ALS has many solutions which are mathematically correct for a
75 given problem, although by proper selection of the initial state and application of natural
76 restrictions, it is possible to find a solution satisfying a real underlying chemical model [30,31].
77 The latter feature may be an advantage, because a better representation of the chromatographic-
78 spectral data should translate into improved analytical performance.

79 In this work, both simulated and experimental second-order liquid chromatographic
80 systems with UV-visible or fluorescence detection are analyzed using PARAFAC2 and MCR-
81 ALS, in order to quantify analytes of interest under conditions of varying complexity (including

82 artifacts of various types and presence of potentially interferent species). The simulation study
83 allows one to critically assess the conditions under which PARAFAC2 is able to model
84 chromatographic changes in peak position and band shapes, visually illustrating the effect of the
85 algorithmic restrictions on retrieved profiles. MCR-ALS was previously compared with
86 PARAFAC2 and other models [32], although in the latter work emphasis was put on the
87 essential step for choosing a suitable resolution method, i.e. determining the inner structure of a
88 three-way array (trilinear or non-trilinear), and specific differences between PARAFAC2 and
89 MCR-ALS were not explored.

90 The selected experimental data correspond to the determination of: (1) various pesticides
91 in fruit and juice samples from liquid chromatography with multi-wavelength UV-visible
92 detection, and (2) polycyclic aromatic hydrocarbons (PAHs) in water samples from liquid
93 chromatography with multi-wavelength fluorescence detection. The first experimental system
94 illustrates the resolution of compounds of environmental concern in foodstuff, such as
95 carbendazim (MBC), thiabendazole (TBZ), propoxur (PRO), fuberidazole (FBZ) and carbaryl
96 (CBL) [33]. The latter was undertaken in view of the growing concern for food safety, as
97 regulated by the European Commission [34] and the Food and Drug Administration [35], among
98 other agencies. The second system encompasses the analysis of PAHs, a large class of ubiquitous
99 aromatic compounds, originated through incomplete combustion of organic matter [36], which
100 are either genotoxic and mutagenic or synergists in causing cancer [37]. The European legal
101 limits for such contaminants were agreed upon by Regulation 1881/2006, fixing a limit for only
102 benzo[*a*]pyrene (BaP), and defining it as a marker for the presence of the remaining PAHs [38].
103 However, the European Food Safety Authority suggested in 2008 the use of the sum of eight
104 PAHs (PAH8), namely benzo[*a*]anthracene, chrysene, benzo[*b*]fluoranthene (BbF),

105 benzo[*k*]fluoranthene (BkF), BaP, dibenzo[*a,h*]anthracene (DBA), benzo[*g,h,i*]perylene (BgP)
106 and indeno[1,2,3-*cd*]pyrene (IcP) [39]. This led to Regulation 835/2011, which fixed new limits,
107 in particular for oils and fats [40].

108 Palpably, the regulations on the identification and/or determination of all these
109 compounds of environmental concern in natural and food samples are constantly updated.
110 Therefore, it is essential to generate improved analytical techniques for their determination in
111 complex matrices. In this sense, the present report indicates that MCR-ALS provides the best
112 analytical results, even in the presence of potential interferents in the test samples, by processing
113 high-performance liquid chromatography coupled to multi-wavelength (UV-visible or
114 fluorescence) spectral detection under isocratic conditions, which notably reduces the analysis
115 time and consumption of organic solvents.

116

117 **2. THEORY**

118 *2.1. Simulations*

119 Data have been synthesized for two systems: (1) simulated System 1, having two
120 calibrated analytes and no interferents in test samples, and (2) simulated System 2, having two
121 calibrated analytes and a single potential interferent in the test samples along with the analytes.
122 All data arrays were built mimicking second-order chromatographic data (elution time-spectral
123 detection), similar to those recorded for the experimental systems.

124 The simulated signal-concentration relationship for component *n* is governed by the
125 following equation:

$$126 \quad \mathbf{M}_n = y_n \mathbf{a}_n \mathbf{b}_n^T$$

127 (1)

128 where \mathbf{M}_n is the $J \times K$ pure-component matrix signal at concentration y_n (J and K are the number
 129 of channels in each mode –time and spectra, respectively– and are both equal to 100), i.e., with
 130 elution times in the columns and spectra in the rows. The product $(\mathbf{a}_n \mathbf{b}_n^T)$ represents a bilinear
 131 pure-component matrix at unit concentration, obtained by multiplying the corresponding profiles
 132 \mathbf{a}_n and \mathbf{b}_n in each data mode (of size $J \times 1$ and $K \times 1$ respectively). In equation (1), the superscript
 133 ‘T’ indicates transposition.

134 Representative Gaussian elution time profiles \mathbf{a}_n ($n = 1, 2$ and 3), partially overlapped in
 135 the time mode, are shown in Fig. 1A, although they change from sample to sample during the
 136 simulations. Various types of chromatographic shifts and band shape changes were introduced
 137 into these time profiles, in order to generate a comprehensive set of cases to be studied. The
 138 intention was to create a trend of growing complexity in the data, in the sense of increasing loss
 139 of trilinearity. This was done to rigorously test the predictive ability of PARAFAC2 and MCR-
 140 ALS towards analyte determination in the test sample sets. To generate the simulated data
 141 affected by the different chromatographic artifacts, the profile \mathbf{a}_n in equation (1) is affected by
 142 sample-specific shifts and broadening effects, as described by the following expression:

$$143 \quad a_n(t, i) = k_{ni} \exp \left[-\frac{4 \ln 2 (t - t_{Rn} - \Delta t_{ni})^2}{(w_n + \Delta w_{ni})^2} \right] \quad (2)$$

144 where t represents each of the time sensors (from 1 to J), t_{Rn} and w_n are the reference retention
 145 time and full width at half height respectively for component n ($t_{R1} = 45$, $t_{R2} = 55$, $t_{R3} = 66$, $w_1 =$
 146 $w_2 = w_3 = 8$, all measured in sensor units), and Δt_{ni} and Δw_{ni} are the sample- and component-
 147 dependent changes in position and width (the subscript i characterizes the sample and n the
 148 component). The value of Δt_{ni} is given by $(r_{ni} \times f \times t_{Rn})$, where r_{ni} is a random number in the range
 149 0-1 (this random number is different for each component in each sample), and f is shown in
 150 Table 1 for each data set. In some cases Δt_{ni} is positive for all samples, while in others Δt_{ni} is

151 randomly positive or negative, as identified as 'S' or 'R' respectively in Table 1. The remaining
 152 parameter Δw_{ni} has been set to zero in some cases (no width changes), or as equal to
 153 $(w_n \times \Delta t_{ni} / t_{Rn})$, with the sign accompanying the changes brought about by Δt_{ni} (i.e., longer
 154 retention times leads to wider peaks and viceversa). Basically, equation (2) means that
 155 chromatographic peaks are shifted in each sample by an amount proportional to the retention
 156 time (f measures the relative degree of change), with a concomitant increase in width which is
 157 proportional to the change in retention time. Supplementary material is provided showing
 158 representative simulated chromatograms.

159

160 **Table 1.** Details for the simulated data sets.

Simulated System 1					Simulated System 2				
Case	f^a	Sign ^b	Δw_{ni}^c	CD ^d	Case	f^a	Sign ^b	Δw_{ni}^c	CD ^d
1	0	No shift	No	0.00	1	0	No shift	No	0.00
2	0.5	S	No	0.04	2	0.25	S	No	0.00
3	0.5	S	Yes	0.10	3	0.25	S	Yes	0.00
4	0.5	R	No	0.13	4	0.25	S	No	0.05
5	0.75	S	Yes	0.15	5	0.5	S	Yes	0.11
6	1	S	Yes	0.18	6	0.25	R	Yes	0.13
7	0.25	R	Yes	0.19	7	0.5	R	Yes	0.18
8	0.75	R	Yes	0.25	8	0.75	S	Yes	0.23
9	1	R	Yes	0.27	9	0.5	R	No	0.28
10	0.75	R	No	0.38	10	0.75	R	Yes	0.36

161 ^a The parameter f controls the relative shift in peak position. ^b Signs of peak shifts: S, positive in
 162 all samples, R, randomly positive or negative depending on the sample. ^c The parameter Δw_{ni} is
 163 the change in peak width, 'No' implies no changes across samples, 'Yes' implies width changes as
 164 described in the text. ^d CD, Complexity Degree (see definition in Section 4.1).

165

166 Table 1 also includes Complexity Degree (CD) values, which will be defined below when
 167 discussing some PARAFAC2 characteristics. The final parameter in equation (2) is k_{ni} , a factor

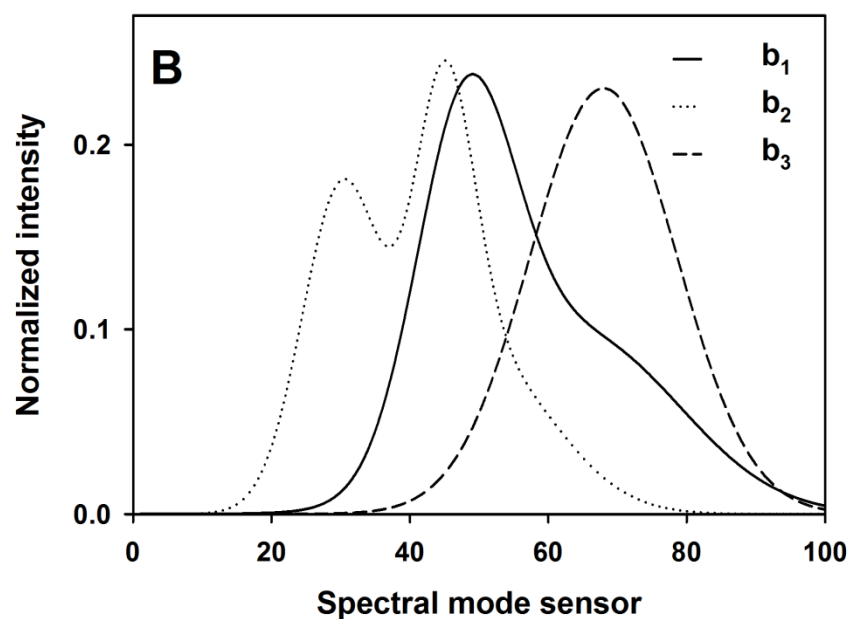
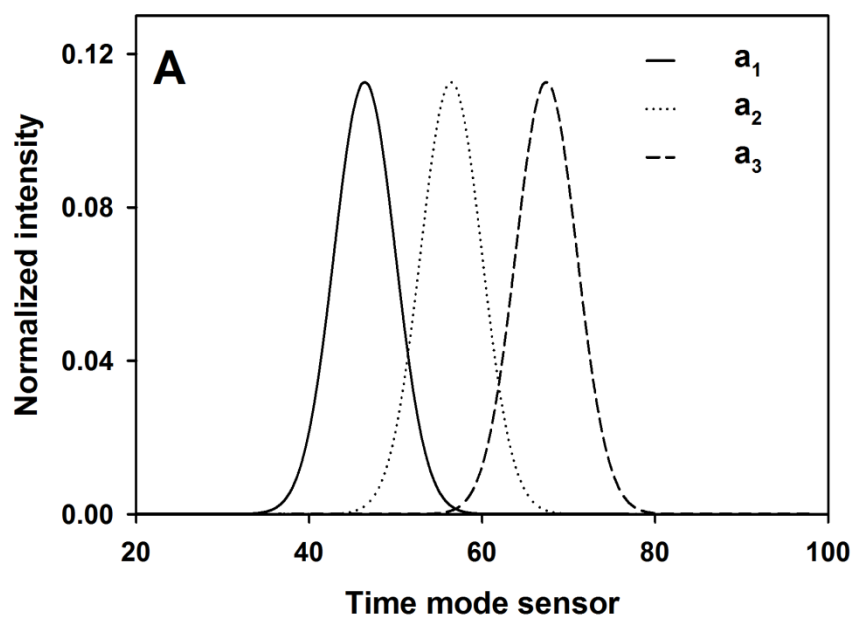
168 employed to scale all elution time profiles \mathbf{a}_n [defined at unit concentration as in eq. (1)] so that
169 the total area under each of them is unitary, since the final time profile for a given component
170 should represent its concentration changes from sample to sample.

171 With regard to the spectral profiles (\mathbf{b}_n) for the sample components, they are shown in
172 Fig. 1B, where considerably overlap can be observed among them. These profiles are normalized
173 to unit length and are common to all samples, as is usual for absorption or fluorescence emission
174 spectra.

175 To produce the calibration data, the matrix signal for a typical sample (\mathbf{X}) is given by the
176 sum of the contributions of both analytes:

$$177 \quad \mathbf{X} = \mathbf{M}_1 + \mathbf{M}_2 \quad (3)$$

178 with \mathbf{M}_1 and \mathbf{M}_2 given by equations analogous to (1) and (2). In all the simulated data sets,
179 calibration samples were created following a 9-sample central composite design with
180 concentrations in the range 0.0-1.0. In the simulated System 1, the analytes were considered to
181 be present in fifty different test samples at concentrations which were taken at random from the
182 range 0.0-1.0. On the other hand, the fifty test samples of simulated System 2 also contained the
183 potential interferent, at concentrations taken at random from the range 0.2-1.5. In this case the
184 test signals were given the sum of three \mathbf{M}_n matrices, each of them provided by equations
185 analogous to (1) and (2). Once the noiseless calibration and test matrices were built, Gaussian
186 noise was added to all signals. The standard deviation was 0.0015 units, representing 1% with
187 respect to the maximum calibration signal of each analyte at unit concentration. The data sets
188 were then submitted to second-order multivariate calibration for the determination of both
189 calibrated analytes as described in the next sections.



190

191 **Fig. 1.** Noiseless profiles employed for the simulations, in the elution time mode (A) and in the
 192 spectral mode (B), for sample components at unit concentration. Solid line, analyte 1, dotted line,
 193 analyte 2, dashed line, potential interferent. The time profiles in (A) are scaled to unit area under
 194 each profile, while in (B) they are normalized to unit length.

195

196

197 2.2. *Second-order multivariate calibration*

198 2.2.2. *Calibration with MCR-ALS*

199 The MCR-ALS model has been discussed in detail elsewhere [41-43] and therefore only
200 a brief description is presented here. In this second-order multivariate method, an augmented
201 data matrix (**D**) is created from each test data matrix and the calibration data matrices. In our
202 case, the direction of columns is represented by the elution time and the direction of rows by the
203 spectra, thus augmentation was implemented column-wise [44].

204 The augmented data matrix **D** is mathematically decomposed into the contribution of
205 individual components [44], assuming a bilinear model which is based on the assumption of the
206 compliance to Beer's law (or its analogues):

207
$$\mathbf{D} = \mathbf{C} \mathbf{S}^T + \mathbf{E} \tag{4}$$

208 where the columns of **D** contain the elution time traces measured for different samples at each
209 spectral sensor. The columns of **C** contain the temporal profiles of the species involved in all the
210 experiments and the rows of **S**^T represent the spectra related to these species. Finally, **E** is the
211 matrix of the residuals not adjusted by the bilinear decomposition, which is performed through
212 alternating least-squares [41].

213 The MCR-ALS algorithm requires an estimation of the number of components
214 responsible for the analytical signal, and initialization with profiles close to the final results. The
215 number of components is usually estimated from principal component analysis of the matrix **D**
216 [41]. On the other hand, the initial spectra of the species can be conveniently estimated from the
217 so-called purest spectral variables [45]. After MCR-ALS decomposition of **D**, concentration
218 information contained in **C** can be used for quantitative predictions, by first defining the analyte
219 score as the area under the elution time profile for the *i*th sample:

$$s(i, n) = \sum_{j=1+(i-1)J}^{ij} c(j, n) \quad (5)$$

where $s(i, n)$ is the MCR-ALS score for component n in sample i . The calibration scores are used to build a pseudo-univariate calibration graph against analyte concentrations, predicting the concentrations of the test sample by interpolation of the test sample score.

225

2.2.3. Calibration with PARAFAC2

PARAFAC2 is performed by joining the training matrices with the unknown sample matrix into a three-way array. This model is a sequel of the original PARAFAC model, which aims at handling shifted, or more generally, varying profiles in a more efficient manner than PARAFAC [23]. If a three-way data set has an ideal trilinear structure, the matrix formulation of PARAFAC can be expressed as:

$$\mathbf{X}_i = \mathbf{A} \mathbf{G}_i \mathbf{B}^T + \mathbf{E}_i \quad (6)$$

where \mathbf{X}_i is the i th frontal slab of the three-way array (a $J \times K$ matrix) containing the elution time profiles (columns) and the spectra (rows) for the i th sample, \mathbf{A} and \mathbf{B} are matrices containing the temporal and spectral loadings, respectively, \mathbf{G}_i is a diagonal matrix holding the relative component concentrations (scores) in its diagonal, and \mathbf{E}_i is a residual matrix. The sum of squared residual elements for all samples is minimized during data processing [46].

In real chromatographic systems, changes in elution time profiles occur among different runs, which can be regarded as a violation of the assumption of parallel proportional profiles underlying the PARAFAC model [46]. The PARAFAC2 approach [29,28] was developed to solve such problems, and its matrix formulation is:

$$\mathbf{X}_i = \mathbf{A}_i \mathbf{G}_i \mathbf{B}^T + \mathbf{E}_i \quad (7)$$

243 where \mathbf{A}_i is the matrix holding the elution profiles of the components present in sample i , and the
244 proposed function to minimize is:

$$\sigma(\mathbf{A}_i, \mathbf{B}, \mathbf{G}_1, \dots, \mathbf{G}_i) = \sum_{i=1}^I \|\mathbf{X}_i - \mathbf{A}_i \mathbf{G}_i \mathbf{B}^T\|^2 \quad (8)$$

247 Initialization is usually performed with the best profiles obtained after 10 runs, each up to
248 a maximum of 80 iterations. Regarding algorithmic restrictions, non-negativity can be applied in
249 the spectral mode (\mathbf{B} profiles), which allows physically interpretable results to be obtained.
250 However, restrictions cannot be easily imposed in the elution time direction when modeling
251 varying chromatographic profiles from sample to sample. This is in contrast to MCR-ALS, in
252 which both spectral and elution time modes can be independently restricted. This may be one of
253 the causes of the better performance of MCR-ALS in the presently studied cases, although an
254 additional PARAFAC2 constraint may be even more relevant in this regard. The latter requires
255 that the cross-product of different \mathbf{A}_i matrices has to be constant over all samples [47]:

$$\mathbf{A}_1^T \mathbf{A}_1 = \mathbf{A}_2^T \mathbf{A}_2 = \dots = \mathbf{A}_i^T \mathbf{A}_i \quad (9)$$

257 The main implication of this latter constraint in PARAFAC2 is that the elution profiles in
258 different experiments may differ (due to peak shifting or band shape changes), but should
259 maintain a similar degree of overlap. As discussed below, this restriction plays a key role in the
260 analytical performance of the PARAFAC2 model.

261 Identification of the chemical constituents under investigation is done with the aid of the
262 estimated profiles, comparing them with those for a standard solution of the analyte of interest.
263 As with MCR-ALS, analyte quantitation is performed in PARAFAC2 by first building a pseudo-
264 univariate calibration line with the analyte scores in the calibration samples (contained in the

265 diagonal of the corresponding \mathbf{G}_i matrix) and then interpolating the analyte score in the test
266 sample. The procedure is repeated for each newly analyzed test sample.

267

268 2.3. Software

269 All calculations were made using in-house MATLAB 7.0 routines [48]. PARAFAC2 was
270 implemented with the codes provided by Bro in his webpage [49]. The routines used for MCR-
271 ALS are freely available on the Internet [50]. All programs were run on an IBM-compatible
272 microcomputer with an Intel Core(TM) i5-2310, 2.90 GHz microprocessor and 16.00 GB of
273 RAM.

274

275 3. EXPERIMENTAL

276 3.1. Experimental System 1: diode array detection

277 This system involves the recently described determination of several pesticides in fruit
278 and juice samples from liquid chromatography with diode array detection (LC-DAD) [33]. The
279 calibration set included 18 aqueous samples of the analytes in the following concentration ranges
280 (in $\mu\text{g L}^{-1}$): MBC, 0-228, TBZ, 0-207, PRO, 0-1720, FBZ, 0-99.2 and CBL, 0-136. The test set
281 involved a total of 20 fruit and juice samples, processed as described in ref. [33], spiked with the
282 analytes with random concentrations, all within the corresponding calibration ranges. All
283 samples were injected into an Agilent HP 1200 liquid chromatograph, using instrumental
284 parameters already reported [33]. The data were collected in the elution time range 0-9.5 min
285 each 1.6 s (356 data points) and spectra were measured in the range 200-350 nm each 1 nm (151
286 data points). The 356×151 LC-DAD matrices were already processed via MCR-ALS [33]. In the

287 present report, a comparison is made with PARAFAC2 predictive results towards four of the
288 analytes, MBC, TBZ, FBZ and CBL, which share similar concentration ranges.

289

290 *3.2. Experimental System 2: fluorescence detection*

291 In this case the analytes BbF, IcP, BaP, DBA, BgP and BkF were determined in water
292 samples in the presence of the potential interferents BjF and BeP, using the chromatographic
293 method developed in ref. [51], i.e., LC with fluorescence spectral detection. The experimental
294 procedure and sample composition were the same as those described in the latter work; therefore
295 they are not repeated here. However, a new data treatment was carried out: from the raw data
296 matrices (collected with the excitation wavelength fixed at 300 nm, using emission wavelengths
297 from 340 to 580 nm each 2 nm, and times from 0 to 7.20 min each 2.7 sec), the temporal mode
298 was restricted to 2.43-7.20 min (matrices were of size 121×111), where coelution of the six
299 analytes mentioned above occurs.

300 The calibration set included 18 samples: 16 corresponded to the concentrations provided
301 by a fractional factorial design at two levels, and the remaining two to a blank and to a solution
302 containing all the studied PAHs at an average concentration. The tested concentrations were in
303 the ranges 0.0-100 ng mL⁻¹ for BbF and IcP, 0.0-50 ng mL⁻¹ for BaP, DBA, and BgP, and 0.0-
304 20.0 ng mL⁻¹ for BkF. The test set contained 20 samples at random concentrations of the studied
305 analytes, including benzo[*j*]fluoranthene (BjF) and benzo[*e*]pyrene (BeP) as interferences (the
306 concentrations of the latter were in the range 0-600 ng mL⁻¹ and 0-1000 ng mL⁻¹, respectively).
307 LC-fluorescence data were collected using a liquid chromatograph equipped with a Waters 515
308 pump connected to a Varian Cary-Eclipse luminescence spectrometer as detector. For additional
309 instrumental details see [51].

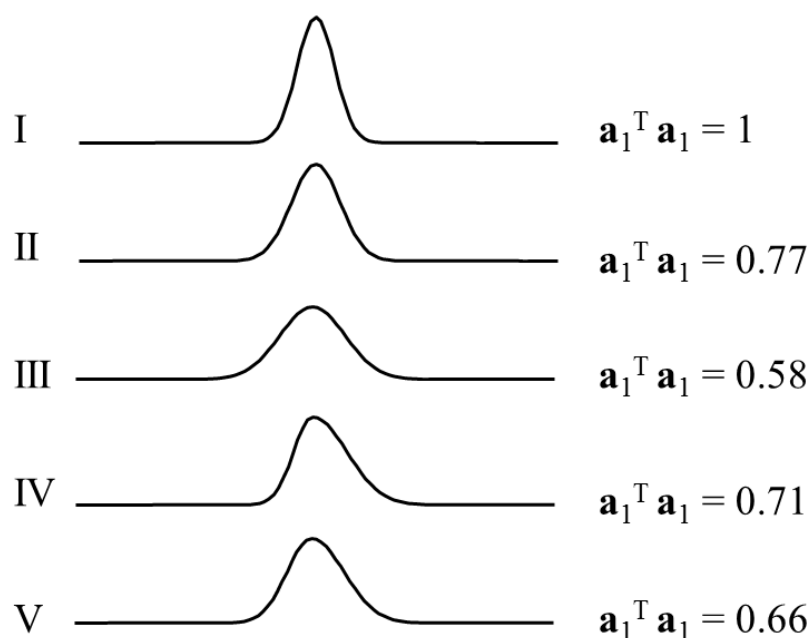
310 4. RESULTS AND DISCUSSION

311 4.1. Intuitive explanation of PARAFAC2 restrictions

312 As discussed above, PARAFAC2 includes an important constraint during least-squares
313 fitting of the three-way data to the model equation (6), i.e., that the cross-products of all \mathbf{A}_i
314 matrices should be equal in all samples. This implies two important consequences: (1) for every
315 sample component n , the squared length of its elution time profile (the value of the product
316 $\mathbf{a}_n^T \mathbf{a}_n$), should be constant across different samples, and (2) for every pair of components, the
317 value of the product $\mathbf{a}_n^T \mathbf{a}_{n'}$ ($n \neq n'$) should also be constant across samples. The latter is
318 proportional to the degree of overlap between elution time profiles: if profiles are normalized,
319 then parallel profiles yield $\mathbf{a}_n^T \mathbf{a}_{n'} = 1$ (full overlap), whereas orthogonal profiles give $\mathbf{a}_n^T \mathbf{a}_{n'} = 0$
320 (null overlap). Intermediate situations lead to degrees of overlap between 0 and 1.

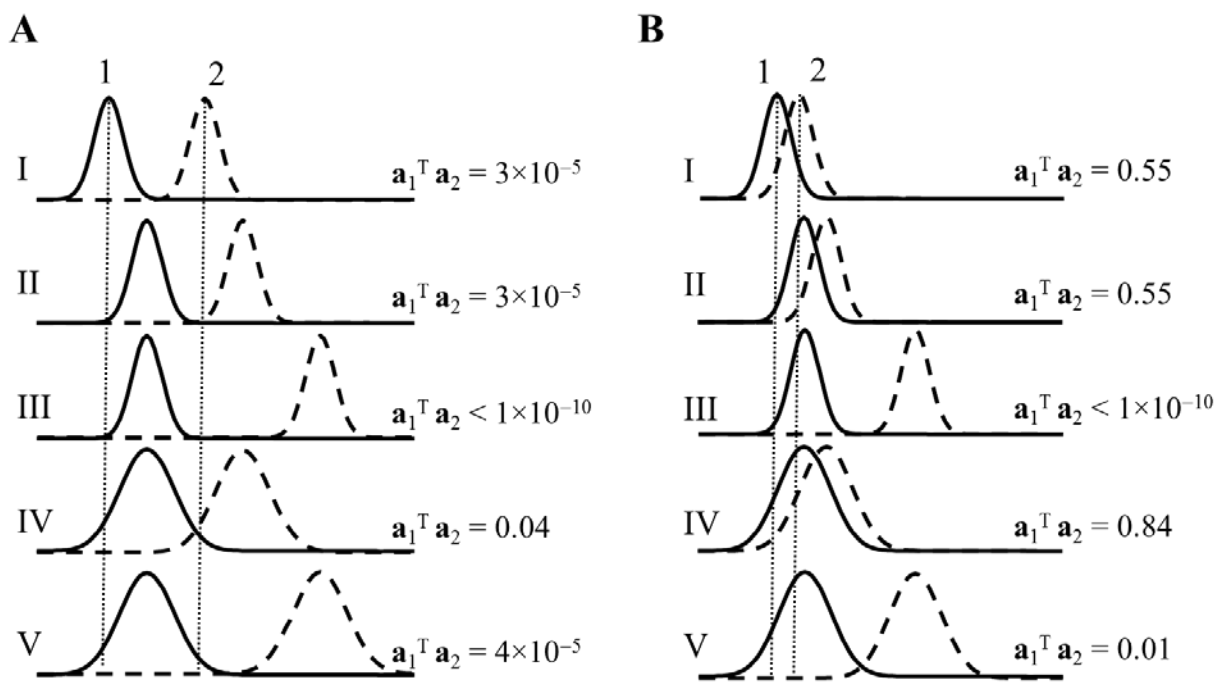
321 These conditions are not universally met under general changes in chromatographic peak
322 positions or shapes. For an illustrative example, Fig. 2 shows the changes in the squared length
323 ($\mathbf{a}_n^T \mathbf{a}_n$) of typical elution profiles for various situations, for a peak of constant area (implying the
324 same component concentration in all cases). In Figs. 2-I, 2-II and 2-III the peak gets wider but
325 maintains the Gaussian shape, while Figs. 2-IV and 2-V display two tailing peaks with different
326 widths. As can be seen, while the peak shapes change, the squared lengths also change, implying
327 that the first requirement of the PARAFAC2 model is not generally met.

328



329

330 **Fig. 2.** Values of the squared length of changing elution time profiles in different
 331 chromatographic runs for a single analyte, keeping the area under the profiles constant.



332

333 **Fig. 3.** Values of the mixed cross-products for changing elution time profiles in different
 334 chromatographic runs for a two-analyte system.

335 As regards the mixed cross-products ($\mathbf{a}_n^T \mathbf{a}_{n'}$, $n \neq n'$), Fig. 3A-I shows two typical
336 Gaussian chromatographic peaks with low overlapping in the elution time direction, for which
337 the cross-product ($\mathbf{a}_1^T \mathbf{a}_2$) is very small. If in a different chromatogram the peak shifts are
338 identical, with no changes in band widths (Fig. 3A-II), the same value of ($\mathbf{a}_1^T \mathbf{a}_2$) will be
339 obtained. For other situations, the product ($\mathbf{a}_1^T \mathbf{a}_2$) will also be small and approximately constant:
340 (1) when the widths are identical but the shifts are different (Fig. 3A-III), (2) when the shifts are
341 equal but the widths are different (Fig. 3A-IV), and (3) when both the shifts and widths are
342 different (Fig. 3A-V). Thus changes in peak positions and widths throughout the different cases
343 illustrated in Figs. 3A-I to 3A-V lead to small changes in the value of the profile cross-product
344 between both components. This means that under low-overlapping condition, the constraint of
345 constant mixed cross-products is verified.

346 Under more serious overlapping in elution profiles, PARAFAC2 will be able to model
347 changes in profiles from sample to sample, only if they satisfy these conditions: (1) changes in
348 peak positions for different components are similar, and (2) no significant changes occur in the
349 profile shapes. This can be visually appreciated in Fig. 3B-I, where two chromatographic traces
350 are shown, overlapped in the elution time direction. For this particular pair of profiles, the degree
351 of overlap ($\mathbf{a}_1^T \mathbf{a}_2$) is 0.55. In a different chromatographic run, illustrated by Fig. 3B-II, the shifts
352 for both peaks are identical, and no changes occur in band widths, leading to the same value of
353 ($\mathbf{a}_1^T \mathbf{a}_2$) as in Fig. 3B-I. This is the ideal situation for the successful application of PARAFAC2.
354 However, for other situations, the product ($\mathbf{a}_1^T \mathbf{a}_2$) may significantly differ from the reference
355 value of 0.55: (1) when the widths are identical for each profile but the shifts are different (Fig.
356 3B-III), (2) when the shifts are equal but the shapes are different (Fig. 3B-IV), and (3) when both
357 the shifts and widths are different (Fig. 3B-V).

358 Comparison of Figs. 2 and 3 leads to the conclusion that the relative changes in
359 overlapping degrees ($\mathbf{a}_1^T \mathbf{a}_2$) may be significantly larger than those in the squared length ($\mathbf{a}_1^T \mathbf{a}_1$),
360 and therefore we propose a measure of the complexity degree (CD) for the various simulated
361 systems, as the standard deviation of the values of ($\mathbf{a}_1^T \mathbf{a}_2$) across the data sets, each involving 59
362 samples (9 calibration and 50 test samples).

363

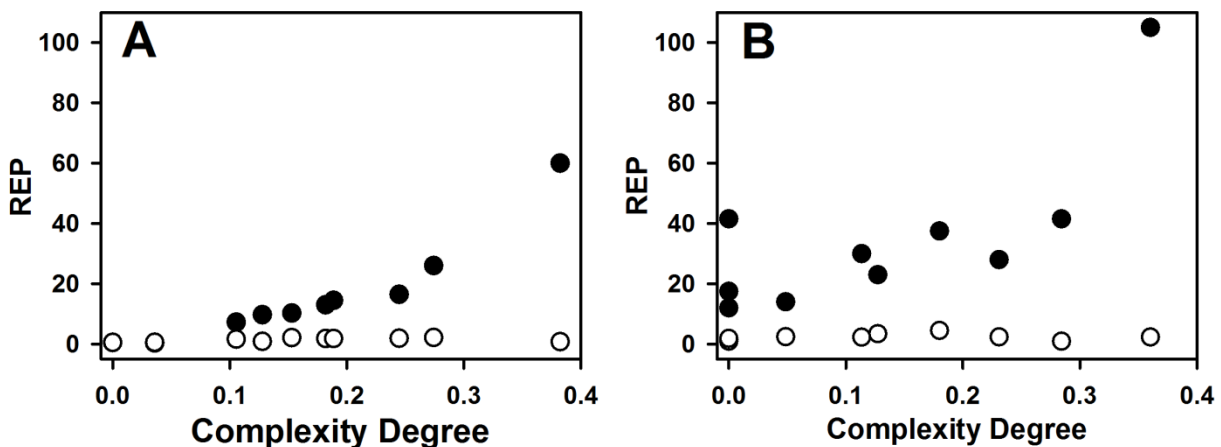
364 *4.2. Results for simulated data*

365 The generation of the simulated data has been described in detail in the relevant Section
366 2.1, with specific values of the CD parameter already provided in Table 1. To process the data,
367 second-order multivariate calibration was performed in order to predict the analyte
368 concentrations in all test mixtures (see Section 2.2). The first model applied to this analytical
369 problem was PARAFAC2 (see Section 2.2.3), considering 2 or 3 components, depending on
370 whether the potential interferent is absent or present in test samples.

371 The results in terms of relative error of predictions (REP) are shown in Fig. 4 for all
372 analyzed cases (Table 1), where REP is defined (in %) as the square root of the mean prediction
373 error, relative to the mean analyte concentration in the calibration set. Specifically for the
374 simulated System 1, where both analytes are calibrated and no potential interferents are present
375 in test samples, the results are collected in Fig. 4A. It is apparent that as the complexity of the
376 system increases, the algorithm performance deteriorates. This appears to confirm that the
377 parameter CD quoted in Table 1, which measures the variability of the cross-product ($\mathbf{a}_1^T \mathbf{a}_2$)
378 across samples, is an adequate indicator of the challenges faced by PARAFAC2.

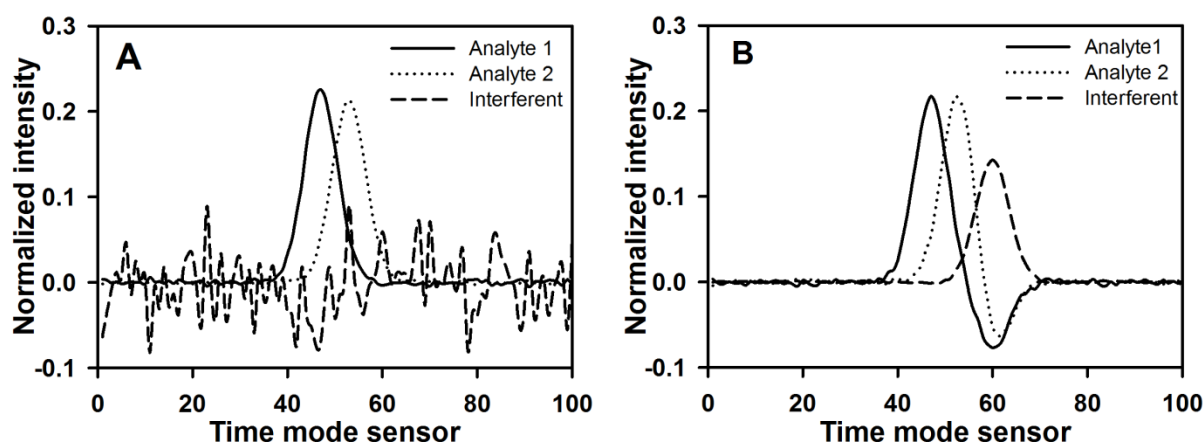
379 On the other hand, for the different cases of the simulated System 2, the corresponding
380 results are shown in Fig. 4B. The correlation of predictive results with the CD parameter is less

381 clear, although it appears that PARAFAC2 finds difficulties in dealing with the presence of the
 382 potential interference, leading to poor analytical results, even in cases where chromatographic
 383 changes are almost negligible. Under these circumstances, the model has serious difficulties in
 384 achieving the second-order advantage.



385
 386 **Fig. 4.** Relative errors of prediction as a function of complexity degree. A) Simulated System 1.
 387 B) Simulated System 2. The REPs are the mean of the predictions for both analytes in the test
 388 sets, and the Complexity Degree is the standard deviation of the mixed cross-products for all
 389 samples [see equation (9)]. The black and white circles correspond to PARAFAC2 and MCR-
 390 ALS results, respectively.
 391

392 When unexpected sample components occur in test samples, the practical effect to restrict
 393 the data set according to equation (9) is shown in Fig. 5. The processing of a typical case of
 394 simulated System 2 via PARAFAC2 yields a rather artificial output for the time profiles of the
 395 test sample (Fig. 5B). They show a compensation effect with respect to a typical calibration
 396 sample (Fig. 5A) through the presence of negative signals. Partially negative analyte profiles are
 397 needed in Fig. 5B to maintain the cross-products $(\mathbf{a}_1^T \mathbf{a}_3)$ and $(\mathbf{a}_2^T \mathbf{a}_3)$ close to zero (1 and 2
 398 correspond to the analytes and 3 to the interferent), as required for a calibration sample (Fig.
 399 5A). It is very likely that this result explains the poor performance of PARAFAC2 for the
 400 simulated System 2 (Fig. 4B).



401
 402 **Fig. 5.** Time profiles retrieved by PARAFCA2 for a calibration sample (A), and for a test sample
 403 (B) during a typical analysis of the simulated System 2.
 404

405 The MCR-ALS model was then applied to these simulated data. In Fig. 4, the prediction
 406 results for the ten cases of Table 1, both in the absence and presence of the potential interferent,
 407 clearly indicate a better performance of this method in comparison with PARAFAC2 for the
 408 quantitation of the analytes. The explanation of the better predictive ability of MCR-ALS relative
 409 to PARAFAC2 should undoubtedly be rooted in the fulfilment of the bilinear chromatographic-
 410 spectral model in the former case, and in the lower flexibility towards chromatographic data in
 411 the latter. This outcome has been previously found in related applications [23,51].

412
 413 *4.2. Results for experimental data*

414 *4.2.1 Experimental System 1*

415 To compare the models discussed in the present report regarding this experimental
 416 system, we have selected the determination of four pesticides in the test samples, all of which
 417 contain potential interferents. The MCR-ALS prediction of the selected analytes MBC, TBZ,
 418 FBZ and CBL, whose concentration ranges are similar, were already provided in ref. [33], and

419 are now graphically shown in Fig. 6A. They lead to root mean square errors of prediction
420 (RMSEP, expressed in $\mu\text{g L}^{-1}$) as follows: MBC, 6.9, TBZ, 5.7, FBZ, 3.8 and CBL, 4.2. This
421 corresponds to REP values (in %) of: MBC, 5.7, TBZ, 5.7, FBZ, 8.9 and CBL, 8.0. When
422 applying the elliptical joint confidence region (EJCR) test to the plot of predicted vs. nominal
423 concentrations for each of the four analytes [52], all ellipses are found to contain the ideal point
424 of unit slope and zero intercept, with small sizes of the elliptical regions (see Supplementary
425 Material). Specific details for the application of MCR-ALS can be found in ref. [33], although it
426 is important to notice that initialization was made with spectral profiles based on purest
427 variables, imposing non-negativity in all profiles and unimodality in elution time profiles for
428 analytes, leaving blank and interfering signals as non-unimodal. The numbers of components
429 considered were 7 or 8 (depending on the sample) in the time range 3.3-6.9 min where MBC,
430 TBZ and FBZ were analyzed, and 4 in the time range 7.3-9.5 min, where CBL was quantitated
431 (in all cases principal component analysis was applied to estimate the number of responsive
432 components). Additional components besides the analytes were due to background signals and
433 unexpected constituents of the test samples.

434 We now report the PARAFAC2 results, obtained by applying non-negativity in spectral
435 profiles and employing the same number of components as for MCR-ALS. The results are shown
436 in Fig. 6B, yielding RMSEP (in $\mu\text{g L}^{-1}$) of 34.1, 31.8, 10.6 and 12.4 for MBC, TBZ, FBZ and
437 CBL respectively, and REP values (in %) of 28.2, 27.2, 25.2, 23.5. These RMSEP values can be
438 statistically compared to those rendered by MCR-ALS using various statistical tests; a suitable
439 one is the randomization test proposed by Van der Voet to compare prediction errors [53]. The
440 result indicates that the RMSEPs found by MCR-ALS are significantly smaller than the ones by
441 PARAFAC2, since the probability values associated to the comparison are smaller than the

442 critical level of 0.05 for the four analytes. When the EJCR test was applied, although for some of
443 the analytes the ideal point is contained within the ellipses, the sizes of the latter regions are
444 considerably larger than those for MCR-ALS described above, indicating significantly poorer
445 precision (see Supplementary Material).

446 This confirms that the PARAFAC2 predictions are considerably worse than those
447 provided by MCR-ALS, a result which can be ascribed to the challenges faced by PARAFAC2
448 constraints for chromatographic profiles, especially when potential interferences appear in the test
449 samples. Indeed, the elution profiles for the interfering components present in fruit and juice
450 samples considerably overlap with all analytes in the working time range (cf. Fig. 5 of ref. [33]).

451

452 *4.2.2 Experimental System 2*

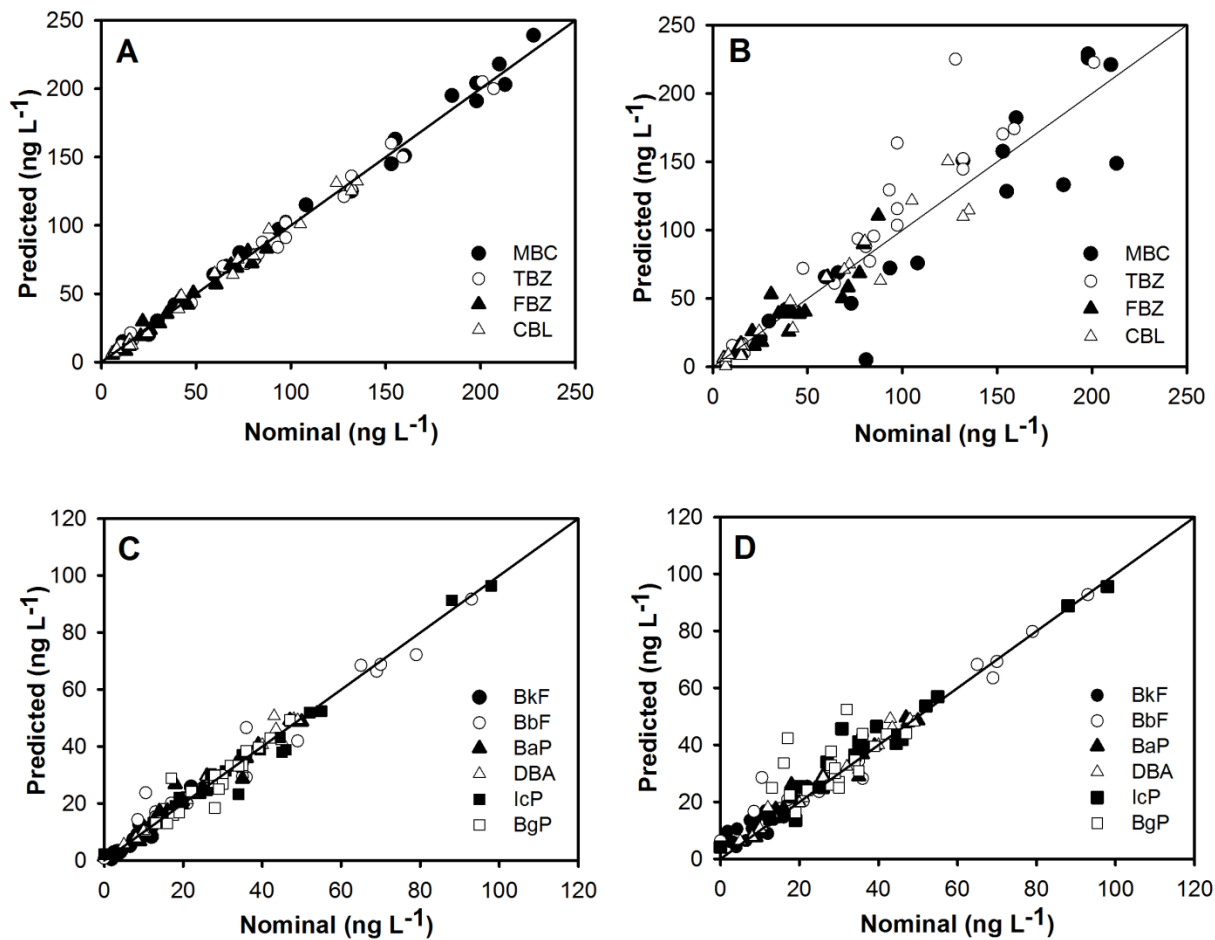
453 These experimental data correspond to the analytical determination of BbF, BkF, BaP,
454 DBA, IcP and BgP in samples which also contain B_jF and BeP as potential interferences. During
455 chromatographic analysis of this series of compounds using fast-scanning fluorescence emission
456 for detection, severe overlapping in both data modes occurred, as illustrated in ref. [51].

457 The general procedure applied to this experimental system was analogous to that
458 discussed above. For MCR-ALS analysis, matrix data for each test sample were augmented with
459 the calibration data matrices and decomposition according to equation (4) was performed by
460 imposing the restriction of non-negativity in both modes and unimodality in the temporal mode
461 (except for a blank signal present in all samples). The number of MCR-ALS components was
462 estimated using a principal component analysis and initialization was performed using the purest
463 spectral variables. The prediction results are shown graphically in Fig. 6C, leading to RMSEP
464 values (in ng mL⁻¹) of 1.5, 5.3, 2.9, 2.3, 3.7 and 3.9 for BkF, BbF, BaP, DBA, IcP and BgP

465 respectively, and REP values (in %) of 15.3, 10.6, 11.0, 9.3, 7.4 and 15.7. It is apparent that the
466 incorporation of potential interferences in the analyzed test analyzed does not preclude a good
467 resolution of the analytical problem, with results comparable to those obtained in reference [51],
468 although the presently discussed MCR-ALS data processing is slightly different. This outcome
469 (i.e., the exploitation of second-order advantage) is consistent both with the abundant
470 experimental evidence [16,26,51,54] as to the assumptions of the model [41].

471 For PARAFAC2, the obtained RMSEP values are 16.2, 14.9, 11.3, 8.5, 9.8 and 13.7 ng
472 mL⁻¹ for BkF, BbF, BaP, DBA, IcP and BgP respectively, with REP% values of 36.0, 51.2, 11.5,
473 10.6, 10.3 and 38.1, indicating that for some analytes the model is not adequate to the problem
474 being analyzed. Indeed, using the same randomization test for comparing RMSEP values
475 mentioned above, the significance of this indicator being larger for PARAFAC2 than for MCR-
476 ALS is confirmed by probabilities which are lower than the critical value of 0.05 for the analytes
477 BkF, BbF and BgP. However, they are larger than 0.05 for BaP, DBA and IcP, suggesting
478 similar predictive ability for the latter three compounds. In agreement with this result,
479 comparison of the EJCRC results for PARAFAC2 and MCR-ALS indicates that the sizes of the
480 ellipses are comparable for BaP, DBA and IcP, but the ones for MCR-ALS are significantly
481 smaller than those for PARAFAC2 in the case of BkF, BbF and BgP (see Supplementary
482 Material). This result is consistent with reference [51], where PARAFAC2 could not be
483 successfully applied when working with the whole chromatogram, which clearly represents a
484 limitation. It is now possible to postulate a reasonable explanation for such behavior:
485 chromatographic artifacts seriously affect the PARAFAC2 modeling of the data, especially when
486 unexpected constituents occur. The comparison of Figs. 6C and 6D visually confirms the better
487 prediction capability of MCR-ALS, although not as significantly as that implied by Figs. 6A and

488 6B for the experimental System 1, most probably as a result of a lower degree of time overlap
489 among analytes and potential interferents in the experimental System 2.



490
491 **Fig. 6.** Plots of predicted concentrations of the studied analytes as a function of the nominal
492 values, in test samples with potential interferences. A) Experimental System 1, MCR-ALS, B)
493 Experimental System 1, PARAFAC2, C) Experimental System 2, MCR-ALS and D)
494 Experimental System 2, PARAFAC2.

495
496 It may be noticed that this same experimental system has been previously studied using
497 both PARAFAC2 and MCR-ALS, dividing the chromatographic axis in various time regions,
498 which were processed separately. In this latter case, PARAFAC2 was reported to yield
499 reasonably good results; however, this mainly refers to those regions where no contribution from
500 the interferents appeared [51]. In the cases where the potentially interferent signals overlapped

501 with those for the analytes in the elution time mode, PARAFAC2 gave worse results in
502 comparison with MCR-ALS, due to the causes discussed in detail in the present paper.

503

504 *4.3. Suggestions for PARAFAC2 improvement*

505 It has been shown that the PARAFAC2 model in its current version is strictly applicable
506 mainly when: (1) there are no potential interferences in test samples, and (2) the changes in peak
507 positions and shapes are moderate, so that the degree of overlapping between all pairs of elution
508 time profiles are approximately constant across experimental runs. One direction in which
509 PARAFAC2 could be improved for the former case, i.e., when unexpected sample components
510 occur in test samples, is to apply some form of sample selectivity or correspondence between
511 components and samples. This will inform the algorithm that the unexpected component is
512 absent in the calibration samples, so that its score can directly be set to zero in the latter ones.
513 The suggested modification might be accompanied by relaxing the need of having, in all
514 samples, a constant cross-product of the interferent time profile with those for any other
515 calibrated component. If these changes can be introduced into the PARAFAC2 model, then it is
516 likely that the latter will improve its predictive ability when the achievement of the second-order
517 advantage is needed.

518

519 **5. CONCLUSIONS**

520 Simulated and experimental second-order liquid chromatographic systems with multi-
521 wavelength (UV-visible or fluorescence) detection were analyzed to show the capability of
522 MCR-ALS and PARAFAC2 to quantify the analytes under study in several problems of diverse
523 complexity. From the simulated systems, it was demonstrated that the cross-product PARAFAC2

524 constraint produces artificial outputs when elution profile changes are severe and/or interferences
525 are present in test samples. The most serious consequence of this phenomenon is that
526 PARAFAC2 cannot achieve the advantage of second-order, even in systems of medium
527 complexity.

528 Experimental examples of MCR-ALS and PARAFAC2 combined to high performance
529 liquid chromatography with multi-wavelength detection were employed to illustrate the rapid
530 resolution of complex mixtures of analytes of environmental concern. The determinations have
531 been carried out even in the presence of unexpected compounds, without the need of a complete
532 chromatographic separation or alignment of elution time traces. In these experimental systems,
533 as well as in the simulated ones, only MCR-ALS led to successful results, which highlights both
534 the power and range of applicability of the latter model.

535

536 **ACKNOWLEDGMENTS**

537 The following institutions are gratefully acknowledged for financial support: Universidad
538 Nacional de Rosario, CONICET (Consejo Nacional de Investigaciones Científicas y Técnicas)
539 and ANPCyT (Agencia Nacional de Promoción Científica y Tecnológica, Project PICT 2010-
540 0084).

541

- [1] H. Parastar, R. Tauler, Multivariate curve resolution of hyphenated and multidimensional chromatographic measurements: a new insight to address current chromatographic challenges, *Anal. Chem.* 86 (2014) 286–297.
- [2] J.M. Amigo, T. Skov, R. Bro, ChroMATHography: solving chromatographic issues with mathematical models and intuitive graphics, *Chem. Rev.* 110 (2010) 4582–4605.
- [3] M.C. Ortiz, L. Sarabia, Quantitative determination in chromatographic analysis based on n-way calibration strategies, *J. Chromatogr. A* 1158 (2007) 94–110.
- [4] J.A. Arancibia, P.C. Damiani, G.M. Escandar, G.A. Ibañez, A.C. Olivieri, A review on second- and third-order multivariate calibration applied to chromatographic data, *J. Chromatogr. B* 910 (2012) 22–30.
- [5] G.M. Escandar, H.C. Goicoechea, A. Muñoz de la Peña, A.C. Olivieri, Second- and higher-order data generation and calibration: A tutorial, *Anal. Chim. Acta* (2013), <http://dx.doi.org/10.1016/j.aca.2013.11.009>
- [6] A. Smilde, R. Bro, P. Geladi, *Multi-way analysis: Applications in the chemical sciences*, Wiley, Weinheim, Germany, 2004.
- [7] A.C. Olivieri, Analytical advantages of multivariate data processing. One, two, three, infinity?, *Anal. Chem.* 80 (2008) 5713–5720.
- [8] B.K. Lavine, J. Workman Jr., *Chemometrics*, *Anal. Chem.* 85 (2013) 705–714.
- [9] S.A. Bortolato, J.A. Arancibia, G.M. Escandar, A.C. Olivieri, Time-alignment of bidimensional chromatograms in the presence of uncalibrated interferences using parallel factor analysis. Application to multi-component determinations using liquid-

- chromatography with spectrofluorimetric detection, *Chemom. Intell. Lab. Syst.* 101 (2010) 30–37.
- [10] K.M. Pierce, B. Kehimkar, L.C. Marney, J.C. Hoggard, R.E. Synovec, Review of chemometric analysis techniques for comprehensive two dimensional separations data, *J. Chromatogr. A* 1255 (2012) 3–11.
- [11] A.C. Olivieri, G.M. Escandar, A. Muñoz de la Peña, Second-order and higher-order multivariate calibration methods applied to non-multilinear data using different algorithms, *Trends Anal. Chem.* 30 (2011) 607–617.
- [12] J.M. Amigo, T. Skov, J. Coello, S. MasPOCH, R. Bro, Solving GC-MS problems with PARAFAC2, *Trends Anal. Chem.* 27 (2008) 714–725.
- [13] J.M. Amigo, M.J. Popielarz, R.M. Callejón, M.L. Morales, A.M. Troncoso, M.A. Petersen, T.B. Toldam-Andersen, Comprehensive analysis of chromatographic data by using PARAFAC2 and principal components analysis, *J. Chromatogr. A* 1217 (2010) 4422–4429.
- [14] M. Vosough, A. Salemi, Exploiting second-order advantage using PARAFAC2 for fast HPLC-DAD quantification of mixture of aflatoxins in pistachio nuts, *Food Chem.* 127 (2011) 827–833.
- [15] R. Tauler, M. Maeder, A. de Juan, Multiset data analysis: Extended multivariate curve resolution, in: T.R. Brown, S.R. Walczak (Eds.), *Comprehensive chemometrics: Chemical and biochemical data analysis*, Elsevier, Oxford (2009), pp. 473–503.
- [16] R.Q. Aucelio, G.M. Escandar, High-performance liquid chromatography with fast-scanning fluorescence detection and multivariate curve resolution for the efficient

- determination of galantamine and its main metabolites in serum, *Anal. Chim. Acta* 740 (2012) 27–35.
- [17] A. Jayaraman, S. Mas, R. Tauler, A. de Juan, Study of the photodegradation of 2-bromophenol under UV and sunlight by spectroscopic, chromatographic and chemometric techniques, *J. Chromatogr. B* 910 (2012) 138–148.
- [18] C. Ruckebusch, L. Blanchet, Multivariate curve resolution: A review of advanced and tailored applications and challenges, *Anal. Chim. Acta* 765 (2013) 28–36.
- [19] Z. Wang, J. Jiang, Y. Ding, H.L. Wu, R.Q. Yu, Trilinear evolving factor analysis for the resolution of three-way multi-component chromatograms, *Anal. Chim. Acta* 558 (2006) 137–143
- [20] T.G. Bloemberg, J. Gerretzen, A. Lunshof, R. Wehrens, L.M.C. Buydens, Warping methods for spectroscopic and chromatographic signal alignment: A tutorial, *Anal. Chim. Acta* 781 (2013) 14–32.
- [21] T. Skov, F. van den Berg, G. Tomasi, R. Bro, Automated alignment of chromatographic data, *J. Chemometr.* 20 (2006) 484–497.
- [22] F. Savorani, G. Tomasi, S.B. Engelsen, icoshift: A versatile tool for the rapid alignment of 1D NMR spectra, *J Magn. Reson.* 202 (2010) 190–202.
- [23] L.G. Johnsen, Processing of chromatographic signals: how to separate the wheat from the chaff, Thesis, Faculty of Science, University of Copenhagen (2013).
- [24] L.G. Johnsen, J.M. Amigo, T. Skov, R. Bro, Automated resolution of overlapping peaks in chromatographic data, *J. Chemometr.* 28 (2014) 71–82.

- [25] F. Marini, R. Bro, SCREAM: A novel method for multi-way regression problems with shifts and shape changes in one mode, *Chemom. Intell. Lab. Syst.* 129 (2013) 64–75.
- [26] M. Vosough, H.M. Esfahani, Fast HPLC-DAD quantification procedure for selected sulfonamids, metronidazole and chloramphenicol in wastewaters using second-order calibration based on MCR-ALS, *Talanta* 113 (2013) 68–75.
- [27] L.W. Hantao, H.G. Aleme, M.P. Pedroso, G.P. Sabin, R.J. Poppi, F. Augusto, Multivariate curve resolution combined with gas chromatography to enhance analytical separation in complex samples: A review, *Anal. Chim. Acta* 731 (2012) 11–23.
- [28] H.A.L. Kiers, J.M.F. ten Berge, R. Bro, PARAFAC2 - Part I. A direct fitting algorithm for the PARAFAC2 model, *J. Chemometr.* 13 (1999) 275–294.
- [29] R. Bro, H.A.L. Kiers, C.A. Andersson, PARAFAC2 - Part II. Modeling chromatographic data with retention time shifts, *J. Chemom.* 13 (1999) 295–309.
- [30] J. Jaumot, R. Tauler, MCR-BANDS: A user friendly MATLAB program for the evaluation of rotation ambiguities in Multivariate Curve Resolution, *Chemom. Intell. Lab. Syst.* 103 (2010) 96–107.
- [31] H. Abdollahi, R. Tauler, Uniqueness and rotation ambiguities in multivariate curve resolution methods, *Chemom. Intell. Lab. Syst.* 108 (2011) 100–111.
- [32] A. de Juan, R. Tauler, Comparison of three-way resolution methods for non-trilinear chemical data sets, *J. Chemometr.* 15 (2001) 749–772.
- [33] V. Boeris, J.A. Arancibia, A.C. Olivieri, Determination of five pesticides in juice, fruit and vegetable samples by means of liquid chromatography combined with multivariate curve resolution, *Anal. Chim. Acta* 814 (2014) 23–30.

- [34] European Commission, <http://ec.europa.eu/>, last accessed on 24th January 2014.
- [35] Department of Health & Human Services. U.S. Food and Drug Administration, <http://www.fda.gov/>, last accessed on 24th January 2014.
- [36] T. Wenzl, R. Simon, J. Kleiner, E. Anklam, Analytical methods for polycyclic aromatic hydrocarbons (PAHs) in food and the environment needed for new food legislation in the European Union, *Trends in Anal. Chem.* 25 (2006) 716–725.
- [37] SCF, Scientific Committee on Food, Opinion of the Scientific Committee on Food on the risks to human health of polycyclic aromatic hydrocarbons in food. 4 December 2002, European Commission, Brussels, 2002.
- [38] European Commission Regulation (EC) No 1881/2006, *Off. J. Eur. Comm.* L364 (2006) 5.
- [39] European Food Safety Authority (EFSA), Polycyclic aromatic hydrocarbons in food, Scientific opinion of the panel on contaminants in the food chain (adopted on 9 June 2008), *The EFSA Journal* 724 (2008) 1–114, http://www.efsa.europa.eu/EFSA/efsa_locale-1178620753812_1211902034842.htm.
- [40] European Commission Regulation (EC) 835/2011, *Off. J. Eur. Comm.* 215 (2011) 4.
- [41] R. Tauler, Multivariate curve resolution applied to second order data, *Chemom. Intell. Lab. Syst.* 30 (1995) 133-146.
- [42] J. Jaumot, R. Gargallo, A. de Juan, R. Tauler, A graphical user-friendly interface for MCR-ALS: a new tool for multivariate curve resolution in MATLAB, *Chemom. Intell. Lab. Syst.* 76 (2005) 101–110.

- [43] M. Jalali-Heravi, H. Parastar, M. Kamalzadeh, R. Tauler, J. Jaumot, MCRC software: A tool for chemometric analysis of two-way chromatographic data, *Chemom. Intell. Lab. Syst.* 104 (2010) 155–171.
- [44] A. de Juan, R. Tauler, Chemometrics applied to unravel multicomponent processes and mixtures. Revisiting latest trends in multivariate resolution, *Anal. Chim. Acta* 500 (2003) 195–210.
- [45] W. Windig, J. Guilment, Interactive self-modeling mixture analysis, *Anal. Chem.* 63 (1991) 1425–1432.
- [46] R. Bro, PARAFAC: Tutorial & applications, *Chemom. Intell. Lab. Syst.* 38 (1997) 149–171.
- [47] R. Bro, Multi-way analysis in the food industry. Models, algorithms, and applications, Ph. D. Thesis, University of Copenhagen (1998).
- [48] MATLAB 7.0, The Mathworks, Natick, Massachussets, USA, 2007.
- [49] <http://www.models.kvl.dk/source/>.
- [50] <http://www.ub.es/gesq/mcr/mcr.htm>.
- [51] S.A. Bortolato, J.A. Arancibia, G.M. Escandar, Non-Trilinear chromatographic time retention-fluorescence emission data coupled to chemometric algorithms for the simultaneous determination of 10 polycyclic aromatic hydrocarbons in the presence of interferences, *Anal. Chem.* 81 (2009) 8074–8084.
- [52] A.G. González, M.A. Herrador, A.G. Asuero, Intra-laboratory testing of method accuracy from recovery assays, *Talanta* 48 (1999) 729–736.

- [53] H. van der Voet, Comparing the predictive accuracy of models using a simple randomisation test, *Chemom. Intell. Lab. Syst.* 25 (1994) 313-323.
- [54] M.J. Culzoni, A. Mancha de Llanos, M.M. de Zan, A. Espinosa-Mansilla, F. Cañada-Cañada, H.C. Goicoechea, Enhanced MCR-ALS modeling of HPLC with fast scan fluorimetric detection second-order data for quantitation of metabolic disorder marker pteridines in urine, *Talanta* 85 (2011) 2368–2374.